

More on a possible energy dependence of Θ_{13} in vacuum neutrino oscillations

Frans R. Klinkhamer*

*Institute for Theoretical Physics,
University of Karlsruhe (TH),
76128 Karlsruhe, Germany*

Abstract

Vacuum neutrino-oscillation probabilities from a simple three-flavor model with both mass-square differences and timelike Fermi-point splittings have been presented in a previous article [hep-ph/0504274]. Here, further results are given: first, for specific parameters relevant to MINOS in the low-energy mode and, then, for arbitrary parameters. A generalized model with equidistant Fermi-point splittings and an additional complex phase is briefly discussed.

PACS numbers: 14.60.St, 11.30.Cp, 73.43.Nq

Keywords: Non-standard-model neutrinos, Lorentz noninvariance, Quantum phase transition

*Electronic address: frans.klinkhamer@physik.uni-karlsruhe.de

I. MODEL

In a previous article [1], we have considered a simple three-flavor neutrino-oscillation model with both mass-square differences (Δm_{ij}^2) and timelike Fermi-point splittings ($\Delta b_0^{(ij)}$). This particular model will be called the “stealth model,” as it allows for Fermi-point-splitting effects hiding behind mass-difference effects.

Setting $\hbar = c = 1$ and writing $p \equiv |\vec{p}|$ for the neutrino momentum, the Hamiltonian of the stealth model contains three terms in the $(\nu_e, \nu_\mu, \nu_\tau)$ flavor basis,

$$H \supset p \mathbb{1} + X D_m X^{-1} + Y D_{b_0} Y^{-1}, \quad (1)$$

with diagonal matrices

$$D_m \equiv \text{diag} \left(\frac{m_1^2}{2p}, \frac{m_2^2}{2p}, \frac{m_3^2}{2p} \right), \quad D_{b_0} \equiv \text{diag} \left(b_0^{(1)}, b_0^{(2)}, b_0^{(3)} \right), \quad (2)$$

and $SU(3)$ matrices

$$X \equiv M_{32}(\theta_{32}) \cdot M_{13}(\theta_{13}, \delta) \cdot M_{21}(\theta_{21}), \quad Y \equiv M_{32}(\chi_{32}) \cdot M_{13}(\chi_{13}, \omega) \cdot M_{21}(\chi_{21}), \quad (3)$$

in terms of the basic matrices

$$M_{32}(\vartheta) \equiv \begin{pmatrix} 1 & 0 & 0 \\ 0 & \cos \vartheta & \sin \vartheta \\ 0 & -\sin \vartheta & \cos \vartheta \end{pmatrix}, \quad M_{21}(\vartheta) \equiv \begin{pmatrix} \cos \vartheta & \sin \vartheta & 0 \\ -\sin \vartheta & \cos \vartheta & 0 \\ 0 & 0 & 1 \end{pmatrix},$$

$$M_{13}(\vartheta, \varphi) \equiv \begin{pmatrix} \cos \vartheta & 0 & +e^{+i\varphi} \sin \vartheta \\ 0 & 1 & 0 \\ -e^{-i\varphi} \sin \vartheta & 0 & \cos \vartheta \end{pmatrix}, \quad (4)$$

and the following parameters:

$$\Delta m_{21}^2 \equiv m_2^2 - m_1^2 = 0, \quad R \equiv \Delta b_0^{(21)} / \Delta b_0^{(32)} \equiv (b_0^{(2)} - b_0^{(1)}) / (b_0^{(3)} - b_0^{(2)}) = 0, \quad (5a)$$

$$\theta_{13} = 0, \quad \theta_{21} = \theta_{32} = \chi_{13} = \chi_{21} = \chi_{32} = \pi/4, \quad (5b)$$

$$\delta = \omega = 0. \quad (5c)$$

With all other complex phases vanishing, there are only two neutrino-oscillation parameters left in the model,

$$\Delta m_{31}^2 \equiv m_3^2 - m_1^2 > 0, \quad \Delta b_0^{(31)} \equiv b_0^{(3)} - b_0^{(1)} > 0, \quad (6)$$

which have been taken positive.

For neutrino oscillations over a travel distance L at high energy $E_\nu \sim p$, there are, then, two dimensionless parameters which completely define the problem, at least for the simple

model considered and matter effects neglected. These neutrino-oscillation parameters can be defined as follows:

$$\rho \equiv \frac{2 E_\nu \hbar c}{|\Delta m_{31}^2| c^4 L} \approx \left(\frac{2.5 \times 10^{-3} \text{ eV}^2/c^4}{|\Delta m_{31}^2|} \right) \left(\frac{735 \text{ km}}{L} \right) \left(\frac{E_\nu}{4.656 \text{ GeV}} \right), \quad (7a)$$

$$\tau \equiv \frac{L |\Delta b_0^{(31)}|}{\hbar c} \approx \left(\frac{|\Delta b_0^{(31)}|}{2.685 \times 10^{-13} \text{ eV}} \right) \left(\frac{L}{735 \text{ km}} \right), \quad (7b)$$

with \hbar and c reinstated. In terms of these parameters, an approximate formula for the vacuum probability $P_{\mu e} \equiv P(\nu_\mu \rightarrow \nu_e)$ is given by [1]

$$P_{\mu e}^{\text{stealth}}(\rho, \tau) \sim (1/2) \sin^2(2 \Theta_{13}) \sin^2 \left(\left[\rho^{-1} + \tau + \sqrt{\rho^{-2} + \tau^2} \right] / 4 \right), \quad (8a)$$

with the following energy-dependent effective mixing angle:

$$\Theta_{13}(\rho, \tau) \sim (1/2) \arctan(\rho \tau). \quad (8b)$$

Recall that, according to Eq. (5b), the bare mixing angle θ_{13} vanishes identically and that, as mentioned above, matter effects are neglected in this approximate model probability [2].

II. RESULTS AND DISCUSSION

In Ref. [1], we have given five figures with model results, three of which may be relevant to T2K or NO ν A and two to MINOS in the medium-energy (ME) mode. Here, we present two more figures, Figs. 1 and 2, which may be relevant to MINOS (baseline $L = 735$ km) in the low-energy (LE) mode, with peak neutrino energy \bar{E}_ν approximately equal to 3.75 GeV and neutrino-oscillation length scale $\bar{L} \equiv 2\pi\bar{E}_\nu/|\Delta m_{31}^2| \approx 1860$ km for $\Delta m_{31}^2 \approx 2.5 \times 10^{-3}$ eV 2 . Figures 1 and 2 show that, if MINOS–LE would be able to place an upper limit of 10 % on the appearance probability $P(\nu_\mu \rightarrow \nu_e)$ at the high end of the energy spectrum ($E_\nu \gtrsim 4$ GeV), this would correspond to an upper limit on $|\Delta b_0^{(31)}|$ of approximately 3×10^{-13} eV (assuming $\tau \leq \pi$, see below).

A further figure, Fig. 3, gives numerical results which illustrate the general behavior of the vacuum probability $P_{\mu e} \equiv P(\nu_\mu \rightarrow \nu_e)$ as a function of the two dimensionless parameters ρ and τ from Eqs. (7ab). Note that we expect $\lim_{\tau \rightarrow 0} P_{\mu e}(\rho, \tau)$ to vanish [pure mass-difference model with $\Delta m_{21}^2 = 0$ and $\theta_{13} = 0$] and $\lim_{\rho \rightarrow \infty} P_{\mu e}(\rho, \tau)$ to be given by $\frac{1}{2} \sin^2(\tau/2)$ [pure Fermi-point-splitting model with $\Delta b_0^{(21)} = 0$, $\Delta b_0^{(31)} \neq 0$, and trimaximal mixing]. The landscape of Fig. 3 can be described as follows: mountain ridges start out at $\rho \gg 1$ and $\tau \approx n_\infty \pi$ for odd integers n_∞ , slope down towards lower values of ρ keeping approximately the same values of τ , and, finally, bend towards lower values of τ (more so for ridges with large n_∞). This topography is qualitatively reproduced by the analytic expression (8).

Figure 4 presents a sequence of constant- τ slices of the vacuum probability $P_{\mu e}(\rho, \tau)$ from Fig. 3. The behavior of $P_{\mu e}(\rho, \tau)$ at $\tau = 2\pi$ (or integer multiples thereof) is quite remarkable, being nonzero only for a relatively small range of energies; cf. the short-dashed curve in the upper right panel of Fig. 4.

Finally, we give two figures, Figs. 5 and 6, with constant- τ slices of the vacuum probability $P_{\mu e} \equiv P(\nu_\mu \rightarrow \nu_e)$ from a generalized model with $\Delta b_0^{(21)}$ equal to $\Delta b_0^{(32)}$ and complex phase $\omega = 0$ or $\pi/4$, the other model parameters being kept at the values (5abc). (For high energies, this model is similar to the pure Fermi-point-splitting model studied previously [3].) In this case, the behavior of $P_{\mu e}(\rho, \tau)$ at $\tau \approx 12$ is quite interesting; cf. the short-dashed curves in the lower right panels of Figs. 5 and 6. At the corresponding distance L for given value of the Fermi-point splitting $\Delta b_0^{(31)}$, the stealth model lives up to its name by evading detection via ν_e appearance, unless the experiment is able to reach down to low enough neutrino energies ($\rho \sim 0.15$). In principle, the way to corner this stealth model would be to use broad-band experiments at *different* baselines, but this may require a substantial effort [4].

ACKNOWLEDGMENTS

It is a pleasure to thank Jacob Schneps for useful discussions and C. Kaufhold for help with the figures.

- [1] F.R. Klinkhamer, “Possible energy dependence of Θ_{13} in neutrino oscillations,” *Phys. Rev. D* **71**, 113008 (2005) [hep-ph/0504274].
- [2] Matter effects from the Earth’s mantle (coherent forward scattering) become important for standard mass-difference neutrino oscillations at energies E_ν of order 10 GeV and travel distances L of order 2500 km. For further details and references, see, e.g., A. Bueno, M. Campanelli, and A. Rubbia, “Physics potential at a neutrino factory: Can we benefit from more than just detecting muons?” *Nucl. Phys. B* **589**, 577 (2000) [hep-ph/0005007] and A. Blondel *et al.*, *ECFA/CERN studies of a European neutrino factory complex*, report CERN-2004-002, April 2004, Chapter 3 [hep-ph/0210192].
- [3] (a) F.R. Klinkhamer, *Neutrino oscillations from the splitting of Fermi points*, *JETP Lett.* **79**, 451 (2004) [hep-ph/0403285]; (b) F.R. Klinkhamer, *Lorentz-noninvariant neutrino oscillations: Model and predictions*, to appear in *Int. J. Mod. Phys. A* [hep-ph/0407200]. Note that the notation for the neutrino dispersion relation in these two articles differs from the one used here and in Ref. [1]. For neutrino oscillations in the pure Fermi-point-splitting model of articles (a) and (b), the different sign of $b_0^{(f)}$ can be compensated by a sign change of the complex

phase. For example, setting $\epsilon = -\omega$ in the exact model probabilities (11a)–(11i) of article (b) reproduces the $\rho \rightarrow \infty$ results presented here.

- [4] As a concrete example, take model parameters $\omega = \pi/4$ and $\Delta b_0^{(31)} = 2\Delta b_0^{(21)} = 3.222 \times 10^{-12}$ eV and consider the *combined* performance of four experiments [5, 6]: the stopped K2K experiment (baseline $L = 250$ km and peak energy $\bar{E}_\nu \approx 1.0$ GeV), the running MINOS experiment ($L = 735$ km and $\bar{E}_\nu \approx 3.75$ GeV, in the LE mode), the planned T2K experiment ($L = 295$ km and $\bar{E}_\nu \approx 0.7$ GeV, for an off-axis beam at 2 degrees), and the proposed NO ν A experiment ($L = 810$ km and $\bar{E}_\nu \approx 2$ GeV, at 14 mrad offset in the ME mode). First, calculate the model predictions for the two current experiments. For K2K, the neutrino-oscillation parameters would be $\tau \approx 4.1$ and $\rho \approx 0.63$, so that a value for $P_{\mu e} \equiv P(\nu_\mu \rightarrow \nu_e)$ of only 1% would be expected [cf. solid curve in upper right panel of Fig. 6], which is consistent with the experimental result [7]. For the MINOS–LE experiment with $\tau \approx 12.0$ and $\rho \approx 0.81$, an equally small probability $P_{\mu e} \approx 1\%$ would be expected [cf. short-dashed curve in lower right panel of Fig. 6], which may be difficult to establish experimentally. [Note that this τ –value corresponding to the MINOS baseline is an order of magnitude larger than the one of Fig. 1.] Hence, the model predictions of the appearance probability $P(\nu_\mu \rightarrow \nu_e)$, for the chosen parameters, would be consistent with a null result from both of these current experiments. Next, turn to the model predictions for the two future experiments. For T2K with $\tau \approx 4.8$ and $\rho \approx 0.38$, a relatively large $P_{\mu e}$ would be expected, around 15% [cf. long-dashed curve in upper right panel of Fig. 6]. Similarly, for NO ν A with $\tau \approx 13.2$ and $\rho \approx 0.39$, $P_{\mu e}$ would be approximately 18%. Hence, the model predictions of the appearance probability $P(\nu_\mu \rightarrow \nu_e)$ would imply a clear signal in these future experiments, at least for the chosen parameters. Of course, the lowest values of $|\Delta b_0^{(31)}|$ could be probed by a neutrino factory with appropriate baselines L up to 12800 km and a broad energy spectrum $E_\nu \approx 10–50$ GeV. For further details on the different experiments, see, e.g., Ref. [6].
- [5] S. T’Jampens, *Current and near future long-baseline neutrino experiments*, in: *Proceedings 6th International Workshop on Neutrino Factories and Superbeams*, edited by M. Aoki, Y. Iwashita, and M. Kuze, Nucl. Phys. B (Proc. Suppl.) **149** (2005), p. 24.
- [6] D.A. Harris, *Superbeam Experiments*, in M. Aoki *et al.*, Ref. [5], p. 34.
- [7] M.H. Ahn *et al.* [K2K Collaboration], *Search for electron neutrino appearance in a 250-km long-baseline experiment*, Phys. Rev. Lett. **93**, 051801 (2004), hep-ex/0402017; K. Kaneyuki, *K2K far detector analysis*, in M. Aoki *et al.*, Ref. [5], p. 119.

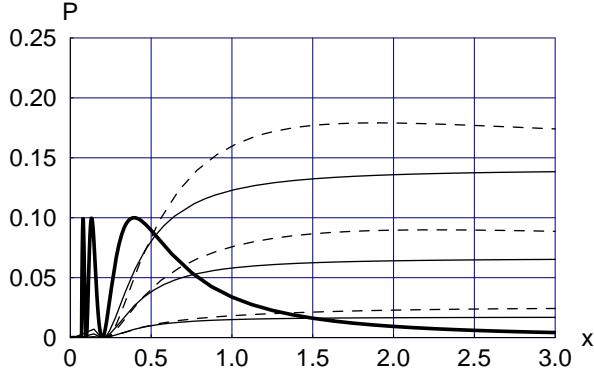


FIG. 1: Fixed-distance vacuum probabilities $P_{\mu e} \equiv P(\nu_\mu \rightarrow \nu_e)$ at $l \equiv L/\bar{L} \equiv L |\Delta m_{31}^2|/(2\pi \bar{E}_\nu) = 735/1860$ vs. dimensionless energy $x \equiv E_\nu/\bar{E}_\nu$ for the “stealth” model of Ref. [1] with both mass differences and timelike Fermi-point splittings, here defined by Eqs. (1)–(6). The broken curves are given by the analytic expression (4.4) of Ref. [1] with parameters $\bar{\Theta}_{13} \equiv \bar{E}_\nu |\Delta b_0^{(31)}|/|\Delta m_{31}^2| = 0.15, 0.30, 0.45$, which correspond to Fermi-point splittings $|\Delta b_0^{(13)}| \approx (1.0, 2.0, 3.0) \times 10^{-13}$ eV for $\bar{E}_\nu = 3.75$ GeV and $\Delta m_{31}^2 = 2.5 \times 10^{-3}$ eV². The same analytic expression is given here by Eq. (8) with parameters $\tau \approx (0.37, 0.74, 1.12)$. These broken curves are only approximate and the corresponding thin solid curves give the full numerical results. The heavy solid curve gives, for comparison, the standard mass-difference probability $P_{\mu e}^{\text{MD}}$ for $\Delta m_{21}^2 = 0$, $\sin^2 \theta_{32} = 1/2$, $\sin^2(2\theta_{13}) = 0.2$, and $l = 735/1860$.

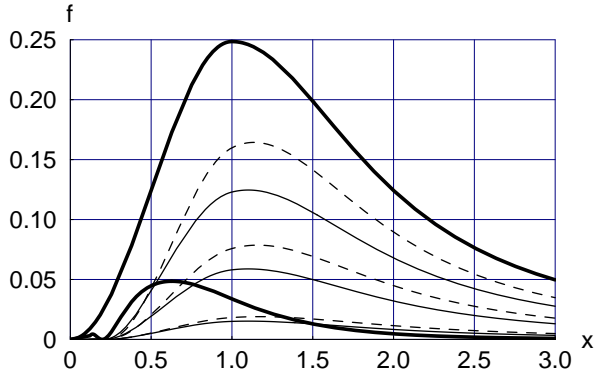


FIG. 2: Electron-type neutrino energy spectra $f_e(x)$ at $l \equiv L/\bar{L} = 735/1860$ from an initial muon-type spectrum (4.8) of Ref. [1] at $l = 0$ and vacuum probabilities $P(\nu_\mu \rightarrow \nu_e)$ of Fig. 1. The initial ν_μ spectrum multiplied by a constant factor 0.25 is shown as the upper heavy solid curve. The ν_e spectra are shown as the thin solid curves [approximate values as thin broken curves] for the stealth model with both mass differences ($\theta_{13} = 0$) and Fermi-point splittings (see Fig. 1 for further details). The lower heavy solid curve gives, for comparison, the ν_e spectrum from the standard mass-difference probability $P_{\mu e}^{\text{MD}}$ for $\sin^2(2\theta_{13}) = 0.2$, as shown in Fig. 1.

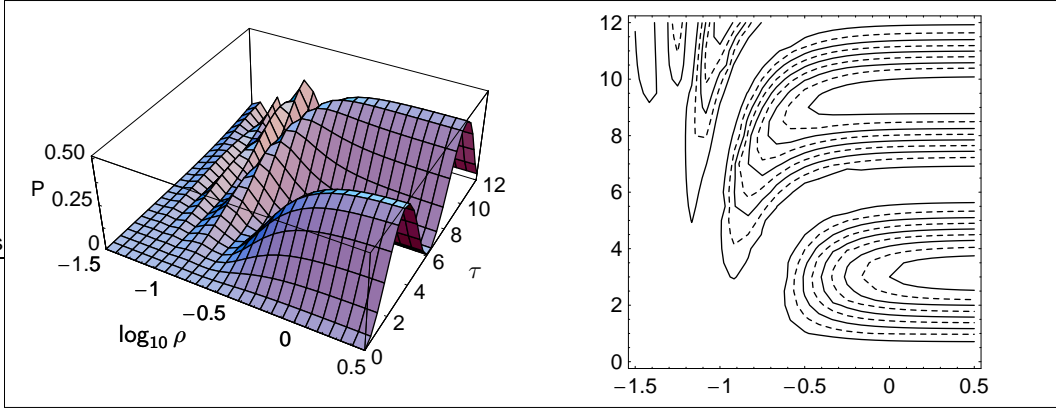


FIG. 3: Numerical results for the vacuum model probability $P_{\mu e} \equiv P(\nu_\mu \rightarrow \nu_e)$ as a function of the two dimensionless parameters ρ and τ , defined by Eqs. (7ab). Left: surface plot. Right: contour plot, with equidistant contours at $P_{\mu e} = 0.05, 0.10, 0.15, \dots, 0.45$ and contours at integer multiples of 0.10 shown dashed.

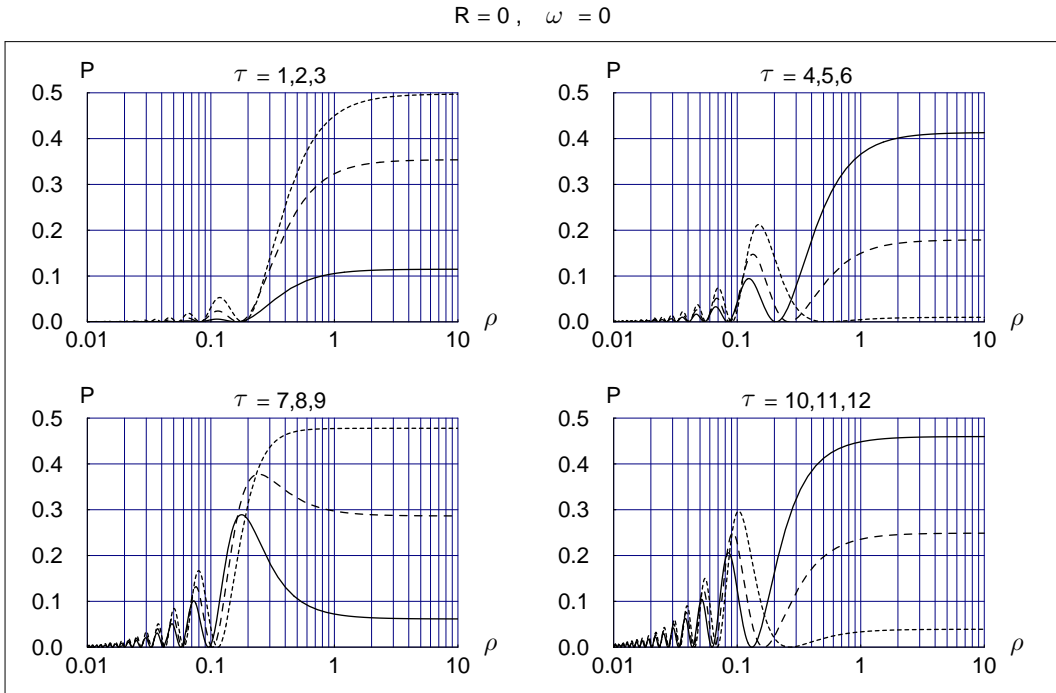


FIG. 4: Numerical results for constant- τ slices of the vacuum probability $P(\nu_\mu \rightarrow \nu_e)$ from Fig. 3. The curves for $\tau = 1, 2, 0 \pmod{3}$ are shown as solid, long-dashed, and short-dashed lines, respectively. For the simple model considered, given by Eqs. (1)–(6), the parameters R and ω vanish identically.

$R = 1, \omega = 0$

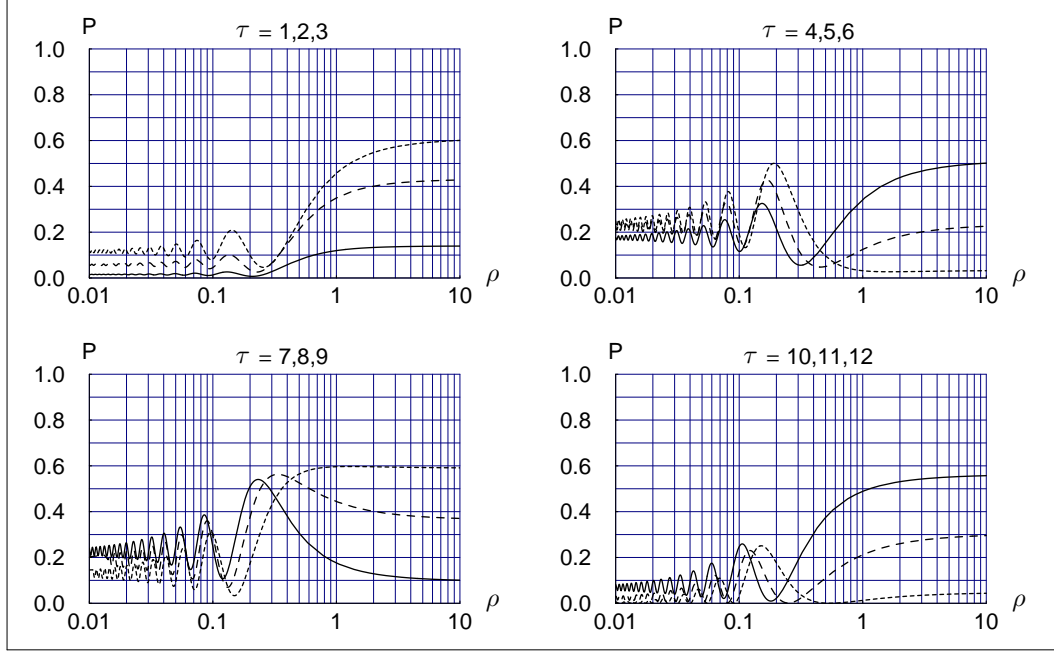


FIG. 5: Numerical results for constant- τ slices of the appearance vacuum probability $P_{\mu e} \equiv P(\nu_\mu \rightarrow \nu_e)$ from the generalized model with ratio $R \equiv |\Delta b_0^{(21)} / \Delta b_0^{(32)}| = 1$ and, just as in Fig. 4, vanishing complex phase ω . The curves for $\tau = 1, 2, 0$ (mod 3) are shown as solid, long-dashed, and short-dashed lines, respectively.

$R = 1, \omega = \pi/4$

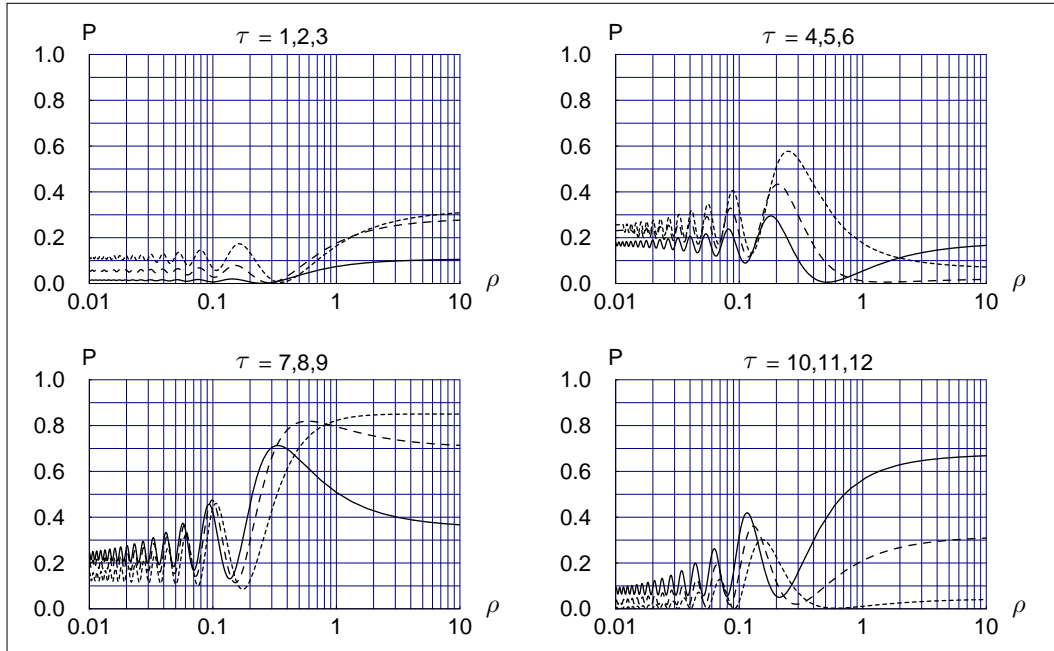


FIG. 6: Same as Fig. 5 but now for $\omega = \pi/4$.